ISA Transactions 96 (2020) 337–351

Contents lists available at ScienceDirect

ISA Transactions

journal homepage: www.elsevier.com/locate/isatrans

Practice article

An experimental case study of robust cascade two-element control of boiler drum level

Sunil P.U. [a,*], Khushali Desai [a], Jayesh Barve [b], P.S.V. Nataraj [c]

[a] GE Power, HTC, Hyderabad, India
[b] GE Global Research Centre, Bangalore, India
[c] Systems and Control Engineering, Indian Institute of Technology Bombay, Mumbai, India

HIGHLIGHTS

- A Quantitative Feedback Theory application for robust boiler drum level control.
- Feasibility study on a laboratory scale natural re-circulation boiler.
- Control performance metric comparison with classical and schedule approach.

ARTICLE INFO

Article history:
Received 20 March 2018
Received in revised form 9 June 2019
Accepted 18 June 2019
Available online 20 June 2019

Keywords:
Boiler-drum level control
Drum type boilers
Heat recovery steam generators
Quantitative feedback theory
Robust control

ABSTRACT

This paper focuses on improving the performance of boiler-drum level control over a wide range of operation using the quantitative feedback theory (QFT) approach. A lab-scale boiler that is a scaled-down version of a power plant boiler is considered for the investigations. The lab boiler has the unique advantage of inducing dynamic variations or uncertainty in system behaviour, to mimic a wide range of real-world operation scenarios. The investigations on the lab boiler are conducted as follows. Firstly, the nonlinear dynamics and uncertainty of the lab boiler over the entire operation envelope are approximated in terms of linear models with parametric variations. Then, a robust two-element QFT control system for drum level control is proposed, designed, and validated over the set of linear models. Next, the proposed QFT controller is implemented on the lab-boiler, and lastly, the performance is compared experimentally with conventional fixed and scheduled two-element control schemes. Comparison of obtained experimental results show that the proposed QFT controller scheme outperforms conventional fixed and scheduled two-element control schemes, for boiler-drum level control over a wide range of operations.

1. Introduction

The state of affairs of power plant operations has been changing in recent years. The increasing penetration of renewable energy sources has caused the slow retirement of less efficient thermal plants. This has led to a paradigm shift regarding operations and dispatch control in the energy sector. Studies conducted by several research groups [1–5] predict the impacts and challenges of renewable energy integration on the power sector. These studies point toward the operational flexibility of thermal power plants for better electrical grid availability and stability. Hence, operational flexibility studies of thermal power plants have become a key topic of increasing interest to academic and industrial researchers [6,7] to address the uncertainty of future generation and loads in the ecosystem. One of the key constituents of a thermal power plant is the boiler and associated subsystem. Under this new paradigm, the boiler system is expected to be more flexible to handle varying loads instead of the traditional fixed base-load or part-load operations. Thus, good performance of boilers across a wide range of operations is an increasingly important control design requirement for power plants.

Boiler drum level is a critical operational parameter which must be maintained for appropriate heat and material balance of the system. Even in a fixed-load operational scenario, boiler-drum level control poses a design and tuning challenge due to its inverse-response behaviour and nonlinearity [8]. Currently, feedback plus feedforward control structures are practised widely in the industry. These structures are popularly known as two-element and three-element controls for drum-type boilers [9]. Traditionally, boiler control is designed and tuned for the full-load operational condition, which traditionally was sufficient because

* Corresponding author.
E-mail addresses: sunil.unnikrishnan@ge.com, sunil@sc.iitb.ac.in (Sunil P.U.), khushali.desai@ge.com (K. Desai), jayeshkumar.barve@ge.com (J. Barve), nataraj@sc.iitb.ac.in (P.S.V. Nataraj).

https://doi.org/10.1016/j.isatra.2019.06.016
0019-0578/

Nomenclature

English Symbols

A	Actuator transfer function matrix
B	QFT bounds
d	Disturbance input
dp	Drum pressure perturbation signal
dl	Drum level perturbation signal
dm	Flow perturbation signal
D	Disturbance transfer function
$\boldsymbol{D}$	Disturbance transfer function set
F	Pre-filter transfer function
G	Controller transfer function
G_w	Feed forward filter
K	Process gain
L	Open loop transfer function
m_{fw}	Feedwater flow
m_s	Steam flow
M_p	Peak overshoot
n	Noise input
P	Plant transfer function
$\boldsymbol{P}$	Plant transfer function set
$\hat{P}$	Process transfer function matrix
s	Laplace variable
t_r	Rise time
t_s	Settling time
T_p	Time constant
T_d	Time delay
T	Closed loop transfer function
T_L	Lower tracking specification
T_U	Upper tracking specification
w	Disturbance process input

Greek Symbols

δ	Perturbated values
λ	Plant parameter vector
ω	Frequency variable
Ω	Finite design frequency set

Suffixes

0	Nominal loop
1	Outer loop
2	Inner loop
12	Inner and outer loop
A	Mode A
B	Mode B
C	Mode C
s	Steam
fw	Feedwater
ff	Feedforward
qft	QFT controller

Abbreviations

2E	Two-element drum level controller
3E	Three-element drum level controller
FT	Flow transmitter
LT	Level transmitter
Mode A	Lab boiler with maximum void in riser
Mode B	Lab boiler with medium void in riser
Mode C	Lab boiler with least void in riser
QFT	Quantitative feedback theory

boilers were seldom operated at part-load, and load-swings were uncommon except during start-up and shut-down. Because of this view, any advancement beyond the traditional three-element control scheme was not widely deployed in the industry. However, the performance of conventional boiler-control degrades in other operation modes, such as start-up, load transitions, and part-load. A study conducted by ASME [10] on a combined-cycle power plant start-up shows that 30% of boiler trips occurring during start-up are due to drum level trip. The study also points to fast load manoeuvring as a reason for trips. Hence, any practical advanced control solution that improves boiler operational flexibility, availability, and efficiency over a wide operational range would be widely welcomed by the industry in the future. To ensure both availability and flexibility, improvement in the performance of drum level control across a wide operational range should be addressed. This is the main motivation of boiler control research work in our paper.

1.1. Overview of boiler control research

In this section, the recent direction in boiler control research is reviewed and presented. Wen Tan et al. [11] explored the practical application of an approximated H_∞ control. This robust control was validated with a nonlinear simulation and the results presented. Chen and Shamma [12] developed a gain-scheduled optimal control system for turbine–boiler dynamics with actuator saturation. The nonlinearity of the system was represented as a linear parameter variation model, and scheduling of control was conducted using drum pressure as an independent variable. Wen Tan et al. [13] designed a simple 2×2 MIMO model and offered a design of coordinated control using a proportional–integral–derivative (PID) controller. Kim et al. [14] illustrated an application of dynamic matrix control (DMC) to a drum-type boiler–turbine system of a fossil power plant. A linear model developed from a nonlinear model and a step response model from plant experiments was used in this approach. A simulation review was performed to validate this notion. A cascade generalized predictive controller (GPC) was proposed and implemented on a 75 MW industrial boiler by Min Xu et al. [15]. A simulation study using DMC for boiler turbine control was performed by Li et al. [16]. A robust decentralized PI control system was proposed by Labibi et al. [17]. The nonlinearity of the boiler was represented as an uncertainty at a nominal plant. Controllers were designed using the IMC method and the results verified in a simulation environment. Zheng et al. [18] explored hybrid control for the full operating range of a coal-fired boiler. An adaptive DMC method was explored by Moon and Lee [19], and the results of a nonlinear simulation presented. Morilla [20] proposed a benchmark of PID control for single-input, single-output (SISO) loops in a boiler. Chen [21] investigated multi-objective control formulation for boiler–turbine dynamics. Variation ranges of drum pressure and tracking magnitude were used as control design parameters based on boiler load ranges. Sliding mode fault-tolerant control was investigated by Saeid Aliakbari et al. [22]. They performed numerical simulations to understand the performance effectiveness of this control and used a fuzzy model to approximate boiler dynamics. A comparison of feedback linearization and gain schedule control was conducted by Moradi et al. [23].

A nonlinear hierarchical model predictive control strategy was proposed by Kong et al. [24]. The approach incorporated both regulatory and economic plant wide operation in an optimization formulation. A state-space model predictive control (MPC) formulization with on-line model linearization and quadratic optimization was explored by Lawrynczuk [25]. A simulation study of marine boiler-drum level control using active disturbance rejection control was conducted by Gan and Bo Lv [26]. Klauco and Kvasnica [27] proposed an MPC based reference for a plant-wide PID controller for a boiler-based thermal power plant.

Most research on boiler controls is limited to simulation-only studies. However, simulation-only studies with almost zero operational data to validate the improvement based on the advancement in control strategy may not help the industry to move forward in the long term. Moreover, researching on real-world boilers is not a viable solution because of the potential risk to the availability of the boiler. Hence, a lab-scale boiler with the capability to mimic a wide range was designed by the authors [28,29]. This scaled-down laboratory boiler was designed and developed to allow experimental control research on boilers, thus giving mutual benefit for industry and academia. In this work, a control law was developed using the framework of a quantitative feedback theory (QFT) [30–32]. This technique, which is based on the concepts of the frequency domain, was expanded further for uncertain plant sets and a nonlinear plant. The nonlinear dynamics associated with a wide range of operations in a boiler were approximated as a linear model with parameter variations. A simulation case study using the QFT approach was explored by the authors [33] and found feasible for further experimental studies. This explored QFT control solution is restricted to maintaining a similar structure to the current industrial boiler-drum level control. The paper focuses on experiments to mimic the current industrial scenario using a two-element drum level control structure (see Appendix B). Reasonable advancement using a scheduled controller and QFT robust control were experimentally studied and are presented here.

1.2. Structure of paper

This paper is divided into five main sections. Section 2 provides an overview and a brief introduction of the lab-scale boiler. Section 3 discusses the experimental cases and the control design for each experiment. Section 4 discusses the results of the experiments. The paper is concluded by summarizing the key observations and outcomes in Section 5.

2. Problem formulation

2.1. Overview and workflow

The central theme of our work is to bring out the advantages of robust control to solve the drum level-control problem, and to motivate the industry to explore this methodology. Real-world operational data would provide greater support for the proposed robust control scheme, ideally from an industrial boiler. However, directly proposing and performing research experiments on any industrial boiler is costly and poses an operational risk. To overcome this, the authors designed and developed a unique laboratory scale boiler with a capability to induce dynamic variations that represent a wide range of operations for an industrial boiler. Moreover, care was taken to ensure that the dynamics and drum-level behaviour and challenges shown by our laboratory-scale boiler mimic and well-represent the behaviour of an industrial boiler.

The experimental plan employed in this work is simple and straightforward. First, we transformed an industrial boiler-drum level-control problem to a laboratory-scale boiler. This was achieved by a unique feature built into the lab boiler which allows the lab boiler to operate in variable void distribution in evaporator tubes with the same heat input. Thus, nonlinearity or dynamic variations due to the wide range of operations in the industrial boiler were transformed as three modes of operation – Mode A, Mode B, and Mode C – in the laboratory boiler. Mode A represents a full steam bubble distribution in the evaporator; hence it can be considered as equivalent to full-load operation. Modes B and C can be considered as part-load operations. Second, an industrial control system was designed at Mode A, and its performance was experimentally evaluated across all three operational modes. This controller is termed the "fixed controller" in this paper. Third, three separate controllers, each designed for the corresponding operational mode, are used. These are termed "scheduled controllers". Last, a robust control law which works well across all three operational modes was designed. The performance of the above three controllers was experimentally evaluated and analysed to draw useful conclusions. Fig. 1 gives a pictorial overview of this study.

To summarize, three control schemes were examined. We designed and tested (1) a traditional fixed-control scheme using classical two-element control designed at mode A and operated at all three modes, (2) a traditional scheduled-control scheme with three separate controllers applied as scheduled control across all three modes, and (3) a proposed QFT-control scheme featuring robust control that works over all the operating regimes using the quantitative feedback theory (QFT) [34–36]. Controllers in each of the above approaches were first designed and then validated using simulations. NI LABVIEW [37] was installed on the data acquisition computer and interfaced with the lab-scale boiler to simulate the controllers for the experiments. Each control scheme was for the three operational modes of the lab-scale boiler. The boiler modes were changed manually using a configuration valve which varied the resistance of the natural recirculation loop.

2.2. Laboratory-scale boiler

This section gives an overview of the laboratory boiler setup which is designed to mimic real-world natural-recirculation-type drum boilers. Fig. 2 shows the laboratory boiler designed and commissioned by the authors [28]. The laboratory boiler has the unique feature of being able to vary the steam bubble distribution by adjusting the circulation ratio. This feature is used to mimic a wide range of real-world operations and introduce uncertainty. The steady-state operation range of the boiler is shown in Table 1. The process variables of interest are the drum pressure and drum level. The variables that can be manipulated to maintain these process variables within the specified tolerance are the steam flow and feedwater flow. In this experiment, the boiler was operated in three modes (based on variable circulation ratio), and these configurations of circulation ratio are termed the three modes of boiler operation: Mode A, Mode B, and Mode C. These three modes represent high bubble distribution, medium bubble distribution, and low bubble distribution in the evaporator, respectively. A wide range of operation dynamics and the transient operation challenge of the industrial boiler was transformed to the experimental boiler with these configurations. Mode A represents the maximum void fraction similar to a base-load condition (100% load) of an industrial boiler and is termed the nominal mode of operation. Modes B and C represent part-load conditions with medium- and low-void fractions. In addition, the boiler can operate at two operating conditions based on the inlet feed water temperature, and these are termed operating point I (cold feed) and operating point II (hot feed), respectively.

The laboratory-scale boiler can be configured as a multi-input, multi-output system like a real-world industrial boiler. In this

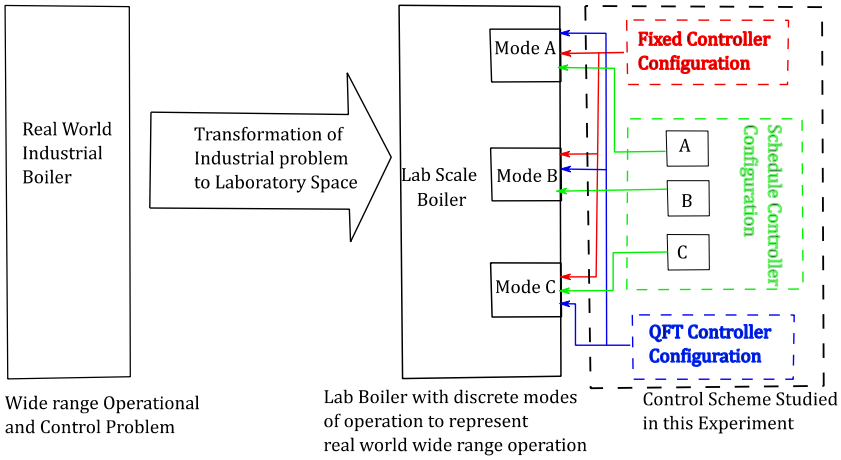

Fig. 1. High-level overview of experimental study.

Fig. 2. Laboratory-scale boiler developed for research work.

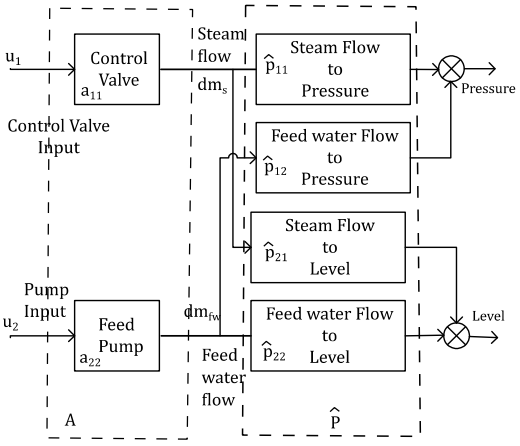

Fig. 3. Block diagram of laboratory boiler system.

Table 1
Operating conditions for laboratory boiler.

Operation parameter	Operation range	Unit
Drum pressure	3.5 to 4.5	bar
Drum level	100	mm
Main heater input	7	kW
Feedwater temperature	90 to 110	C
Feedwater flow rate	8 to 12	l/h
Steam flow rate	8 to 12	kg/h

study, drum pressure and drum level were configured as primary controlled process variables of interest. Drum level was controlled by manipulating feedwater flow, and drum pressure was controlled by manipulating the steam flow rate. In the system, a feed water pump and main steam-flow control valve act as actuators to manipulate feedwater flow and steam flow, respectively. Fig. 3 shows the block diagram of lab boiler configured in this study: $\widehat{p}_{11}$ represents the steam flow to pressure dynamic model, and $\widehat{p}_{12}$ represents the feedwater flow to pressure dynamic model. Similarly, $\widehat{p}_{21}$ and $\widehat{p}_{22}$ represent the steam flow to level and the feedwater to level dynamic models, respectively. For the ease of analysis, these models are represented as a matrix $\widehat{P}$. On the other hand, A represents the actuator model of this laboratory scale boiler, a_{11} represents the steam valve model, and a_{22} represents the pump model. Table 2 shows the range and specification of the control actuator in the lab boiler setup. In this work, the non-linear dynamics of the lab boiler across the operation envelope is represented as a linear model with parametric variations. The next section gives details of these linear models.

2.2.1. Linear model envelope

A detailed system identification design of experiments was performed to identify control-oriented models. The operation envelope of the laboratory boiler is represented as a linear model with parameter variations (LPV). The entire operating regime of the laboratory boiler, which includes the three modes and two operation points, are represented as a set of linear models. A wide range of dynamic variations (at the three modes A, B, C and the two operating points) is transformed into parametric variations over bounded intervals, to enable a QFT design methodology. The laboratory boiler linear model relating the controller outputs (that is, actuator inputs) to pressure and level output variables can be expressed by Eq. (1).

$$\begin{bmatrix} dp \\ dl \end{bmatrix} = [\hat{P}][A] \begin{bmatrix} u_1 \\ u_2 \end{bmatrix} \tag{1}$$

Table 2
Actuator and sensor specifications.

Actuator/ Sensor	Control signal range	Engineering range	Type	Characteristics
Control valve	4–20 mA	0–32 kg/h	Globe 2 way motorized	Equal percentage
Feedwater pump	4–20 mA	0–40 l/h	Plunger pump with motorized actuator	Linear
Drum pressure	4–20 mA	0–10 bar		Linear
Drum level	4–20 mA	0–200 mm		Linear
Feedwater flow	4–20 mA	0–40 kg/h	Rotameter	Linear

Table 3
Lab boiler process model set.

Model name	Model structure	Parametric interval
$\hat{p}_{11}(s)$	$\frac{K}{(T_{p1}s+1)}$	$K \in [-0.9, -2.5]$, $T_{p1} \in [1800, 4600]$
$\hat{p}_{12}(s)$	$\frac{Ke^{-T_d s}}{(T_{p1}s+1)}$	$K \in [-0.09, -0.35]$, $T_{p1} \in [900, 8000]$ and $T_d = 6$
$\hat{p}_{21}(s)$	$\frac{K(s+b)}{s(s+a)}$	$K \in [0.01, 0.2]$, $a \in [0.01, 0.4]$ and $b \in [-0.002, -0.004]$
$\hat{p}_{22}(s)$	$\frac{Ke^{-T_d s}}{s(s+b)(s+c)}$	$K \in [1.53 \times 10^{-5}, 0.1874]$, $b \in [0.0053, 0.7583]$, $c \in [0.1, 52]$, and $T_d \in [2, 6]$

Table 4
Actuator model set.

Model name	Model structure	Parametric interval
$a_{11}(s)$	$K\frac{e^{-T_d s}}{T_p s+1}$	$K \in [0.25, 0.3]$, $T_d = 6$ and $T_p \in [17, 19]$
$a_{22}(s)$	$K\frac{e^{-T_d s}}{T_p s+1}$	$K \in [0.3, 0.42]$ $T_p \in [5, 10]$ and $T_d \in [3, 6]$

where the matrix $\hat{P}$ represents the process transfer function, and the matrix A (a diagonal matrix) represents the transfer function of the actuators—that is, the pump and control valves. The above equation can be written as two separate equations. The first equation is between matrix $\hat{P}$ and flows; the corresponding equation is shown in Eq. (2), where dm_s and dm_{fw} represent the flow deviations.

$$\begin{bmatrix} dp(s) \\ dl(s) \end{bmatrix} = \begin{bmatrix} \hat{p}_{11}(s) & \hat{p}_{12}(s) \\ \hat{p}_{21}(s) & \hat{p}_{22}(s) \end{bmatrix} \begin{bmatrix} dm_s(s) \\ dm_{fw}(s) \end{bmatrix}. \tag{2}$$

In the above, $\hat{p}_{11}$ represents a linear model relating steam flow to drum pressure, and $\hat{p}_{12}$ represents a linear model relating feedwater flow to drum pressure. Similarly, $\hat{p}_{21}$ and $\hat{p}_{22}$ represent a linear model relating steam flow to drum level and feedwater flow to drum level, respectively. Experiments were conducted for identifying these models at various operating modes. Fundamental system identification techniques were used for this purpose, and these models were thoroughly validated with other test operation experiments. Table 3 shows process models identified for the laboratory-scale boiler from system identification experimental studies. Steam flow to drum pressure ($\hat{p}_{11}(s)$) is a first order dynamics and steam flow to level ($\hat{p}_{21}(s)$) is an integrating with right half zero dynamics. Whereas feedwater flow to level model is having double integrator ($\hat{p}_{22}(s)$) one pole at the origin of s-plane and another close to the origin of s-plane) dynamics.

Similarly, the actuator matrix [A] in the MIMO model, Eq. (1), can be expressed using Eq. (3). The dynamics of flow deviations – that is, dm_s and dm_{fw} – are captured in this model.

$$\begin{bmatrix} dm_s(s) \\ dm_{fw}(s) \end{bmatrix} = \begin{bmatrix} a_{11}(s) & 0 \\ 0 & a_{22}(s) \end{bmatrix} \begin{bmatrix} u_1(s) \\ u_2(s) \end{bmatrix} \tag{3}$$

where $[A]$ is a diagonal matrix, in which a_{11} represents the control valve model and a_{22} represent the pump model; see Table 4.

To summarize, the laboratory boiler can be represented as a set of transfer function matrices covering the dynamics of the entire operating envelope; that is, over Mode A, Mode B, and Mode C configurations at two operating points.

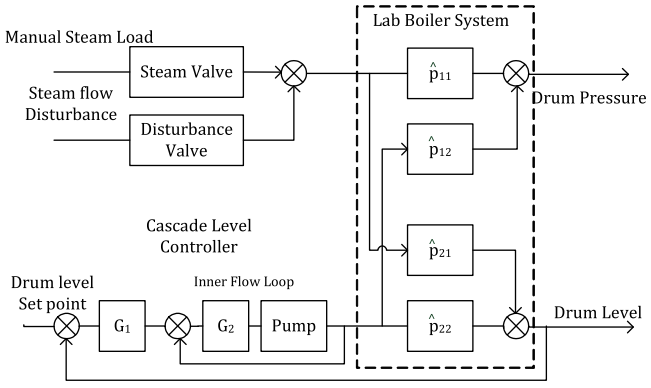

Fig. 4. Control scheme for two-element (SISO) of laboratory boiler.

3. Control design for experimental study

This section covers control design for each control law used in the lab boiler. Fig. 4 shows the two-element control scheme block diagram configured on the laboratory boiler for this experiment. This block diagram shows the configuration of the boiler for the two-element case study. A cascade control loop must be designed: G_1 and G_2 represent the outer and inner flow control loop, respectively. Feedwater flow to the boiler drum is adjusted using the control; final control actuation is on a positive displacement pump. On the steam load side, two manipulations are possible: a steam control valve and a manual disturbance injection valve. Since the current study focuses on the SISO loop, a steam control valve is fixed at a static load position, while the steam load disturbance is provided using a disturbance injection valve.

Generally, this drum level-control structure is tuned for base load or design load conditions. The wide range of operations found in an industrial boiler were mimicked in the laboratory boiler using three modes of configuration, as explained. In this experiment, three control methods were applied on the laboratory boiler: (1) fixed control, (2) schedule control, and (3) QFT-based robust control. The details of the control design investigated on the laboratory boiler are described below.

(a) Fixed control:

This control scheme represents the two-element control scheme currently practised in industry; that is, a single control for all operations. To mimic and study the performance of this scenario on the laboratory boiler, a controller was designed at

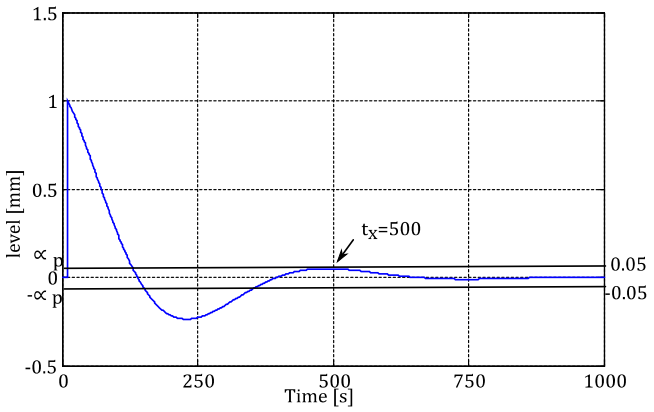

Fig. 5. Disturbance rejection specification for level control.

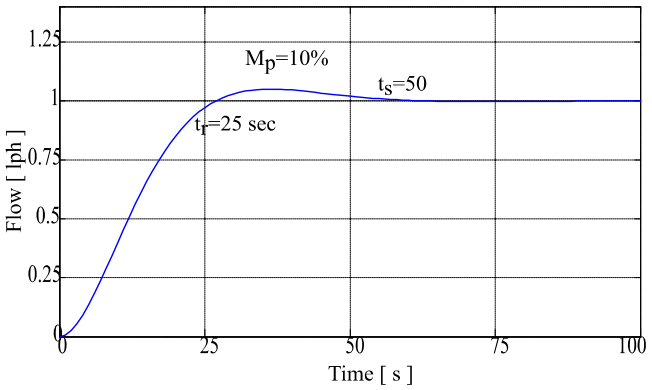

Fig. 6. Tracking specification for the inner flow loop.

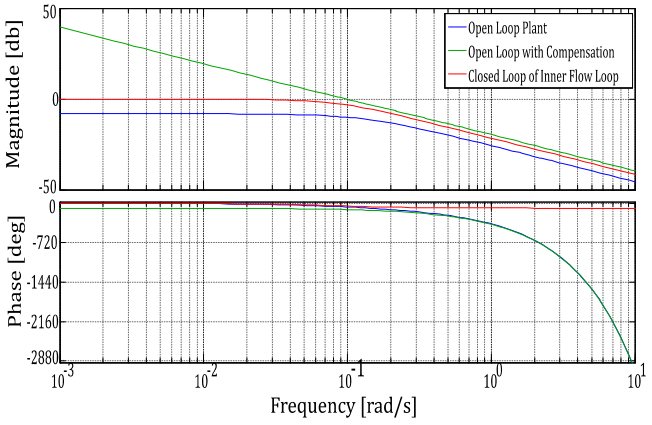

Fig. 7. Bode plots of inner loop design for fixed controller at Mode A. (Blue is open loop plant, green open loop with compensation and red closed loop). (For interpretation of the references to colour in this figure legend, the reader is referred to the web version of this article.)

nominal mode, mode A. Then, the performance of this controller was examined at other modes: Mode B and Mode C.

(b) Scheduled control:

This control scheme represents a schedule control from an industrial perspective. Three separate controllers were designed for each mode, and their performance was evaluated.

(c) QFT-based robust control:

A single robust control scheme was designed for the entire operating envelope using the QFT control design philosophy. The performance of this controller was studied at three modes of laboratory boiler operation. The controller performance obtained with the three schemes was studied in detail.

A steam valve was used to provide load to the boiler, and a small disturbance valve was used to inject disturbance to the system. The disturbance rejection specification for level control for a step steam disturbance is as shown in Fig. 5. The performance of the level controller was evaluated for the three control schemes.

3.1. Fixed control scheme

The fixed controller scheme represents a typical industrial case in which controllers are designed (or tuned) based on 100% guaranteed load conditions, or a maximum continuous rating (MCR) condition, and also allowed to operate at part-load scenarios. In this experimental case study, a control design was performed with models identified at Mode A configuration. Then, the performance was analysed at other configuration modes (viz Modes B and C). The rationality to choose Mode A as the nominal case is because of the maximum void fractions in riser tubes similar to the MCR conditions of industrial boilers.

3.1.1. Inner loop design

The inner loop control (see Fig. 4) is a flow loop with a simple PI control to track flow set point provided by the outer loop. The control Specification for the inner flow loop is given in Fig. 6. The pump transfer function used to design the inner loop is shown in Eq. (4). A loop-shaping technique of the frequency domain design method is used to design the inner loop compensation. The method is based on the idea of choosing a compensation that gives a loop transfer function with the desired shape. One possibility is to start with the loop transfer function of the process and modify it by changing the gain and adding poles and zeros to the controller until the desired shape is obtained. In this work, the Bode loop shaping method [38] with an interactive tool from Math work's control system toolbox [39] is used for the systematic design of classical SISO feedback systems. Fig. 7, shows the open loop, closed loop, and open loop with compensation Bode plot for the inner loop. The control structure and the transfer function of the controller is shown in Eq. (5).

$$P_{2A}(s) = e^{-5.5s}\frac{0.39}{(7.5s+1)} \tag{4}$$

$$G_{2A}(s) = (2 + \frac{0.25}{s}) \tag{5}$$

3.1.2. Outer loop design

The outer loop with the previously designed inner loop block diagram (see Fig. 4). Eq. (6) represents the plant model at Mode A. A simple proportional–integral (PI) control design for disturbance rejection specification (see Fig. 5) was performed. The Bode loop shaping technique [38] was used for designing the controller, and MathWork's interactive control design toolbox [39] was used for the loop shaping. The Bode plot for control design is shown in Fig. 8. The plant model (6) and the corresponding shaped or designed controller are given in (7).

$$P_{1A}(s) = e^{-6s}\frac{0.0014395}{s(s+3.226)(s+0.09515)} \tag{6}$$

$$G_{1A}(s) = (2.7 + \frac{.013}{s}) \tag{7}$$

where $P_{1A}(s)$ represents feedwater to the level transfer function at Mode A, and $P_{2A}(s)$ represents the inner loop: that is, pump transfer function. Similarly, $G_{2A}(s)$ and $G_{1A}(s)$ represent the inner and outer control transfer functions, respectively.

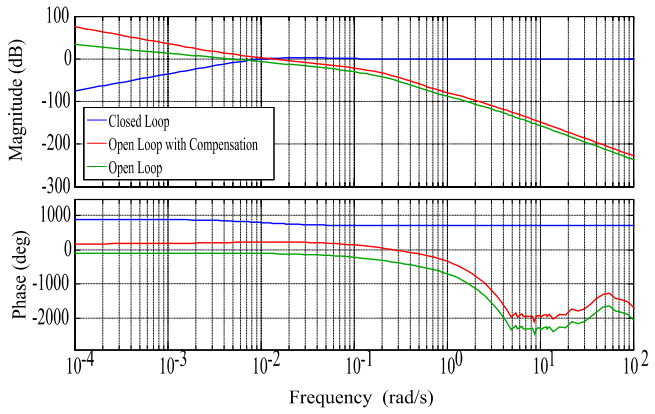

Fig. 8. Bode plots of outer loop design with fixed control (Mode A). (Green is for open loop plant; red is for open loop with compensation, and blue is for closed loop). (For interpretation of the references to colour in this figure legend, the reader is referred to the web version of this article.)

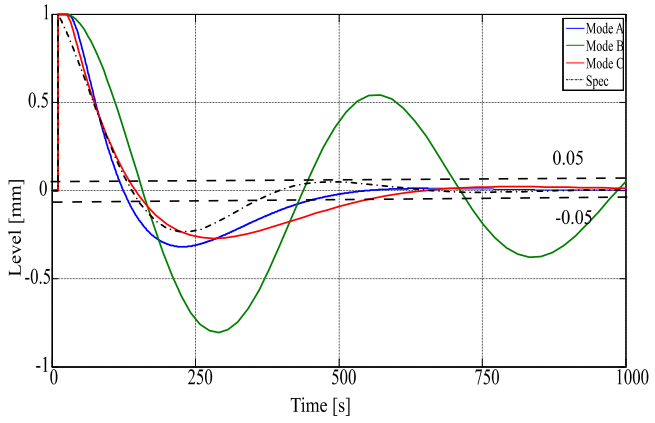

Fig. 9. Closed-loop responses of cascade level control with fixed controller. (Blue is Mode A; Green is Mode B; Red is Mode C; and dotted black is specification).

The simulation validation of the above designs was performed via simulation using MATLAB/Simulink [40]. Linear models of each mode (i.e., A, B, and C) were simulated with a fixed control scheme. A unit step disturbance was provided at the output of the system model. Each plant model – Mode A, B, and C – was simulated independently with a fixed controller. Note that the performance of this fixed control deteriorates at other modes; see Fig. 9.

3.2. Schedule control scheme

In this work, schedule control is the terminology used to represent separate control constants for different modes of operation. This scheme mimics gain (or control constant) scheduling in a real-world industrial application. In the previous section, the control was designed for Mode A. Similarly, two more controls were designed for Modes B and C, with the same control specification. When the boiler is operated in each mode, the respective controller is enabled. Hence, this design and experiment represents a schedule control over a wide range of operation similar to that for an industrial boiler. This section covers the design and verification of schedule control design using a classical control scheme.

3.2.1. Inner loop

Mode A: The same controller designed in the previous section (fixed case) was used.

Mode B: Inner loop control is a flow loop with a simple PI control to track flow set point provided by the outer loop. An average transfer function was used to design the inner loop, shown in Eq. (8). The control specification is the same as that used for fixed control. Fig. 10(a) shows the open loop, closed loop, and open loop with compensation Bode plot for the inner loop. The controller transfer function is shown in Eq. (9).

$$P_{2B} = e^{-6s}\frac{0.38}{(9.6s+1)} \tag{8}$$

$$G_{2B}(s) = (2 + \frac{0.25}{s}) \tag{9}$$

Mode C: The inner loop control is a flow loop with a simple PI control to track the flow set point provided by the outer loop. An average transfer function was used to design the inner loop; see Eq. (10). The specification is the same as that used for fixed control. Bode loop shaping was used for design compensation, as explained in the earlier design. Fig. 10(b) shows the open loop, closed loop, and open loop with compensation Bode plot for the inner loop. The control structure and transfer function used for the design were according to Eq. (11).

$$P_{2C} = e^{-6s}\frac{0.37}{(8.9s+1)} \tag{10}$$

$$G_{2C}(s) = (2 + \frac{0.25}{s}) \tag{11}$$

To summarize, the inner loop has a simple PI control. The variation of pump dynamics with respect to mode and operation change is not very significant. Hence, the controller constants are nearly the same for all the modes (see Eqs. (7), (9), and (11)).

3.2.2. Outer loop

This section presents the outer loop design for Mode B and Mode C.

Mode A: The same controller designed for the fixed controller case was used.

Mode B: The control design employed is that for a disturbance rejection specification described earlier in the fixed control design section. The Bode loop shaping method [38] was used for designing compensation. The Bode plot of the shaped open-loop system with an uncompensated open-loop system is shown in Fig. 11(a).

$$P_{1B}(s) = \frac{5.0099 \times 10^{-05}}{s(s+0.1011)(s+0.1029)} \tag{12}$$

$$G_{1B}(s) = (3.4 + \frac{0.03}{s}) \tag{13}$$

where $P_{1B}(s)$ (Eq. (12)) represents the feedwater to level transfer function at Mode B, and $G_{1B}(s)$ (Eq. (13)) and $G_{2B}(s)$ (Eq. (9)) represent inner and outer control transfer functions, respectively.

Mode C: The control design is for a disturbance rejection specification described earlier in the fixed control design section. Eq. (14) shows the model; Eq. (15) shows the respective control after the loop-shaping outer loop. The Bode plot of the compensated open-loop system with an uncompensated open-loop system is shown in Fig. 11(b).

$$P_{1C}(s) = e^{-3s}\frac{0.0070153}{s(s+0.03025)(s+42.16)} \tag{14}$$

$$G_{1C}(s) = 2.2 + \frac{0.0055}{s} \tag{15}$$

where $P_{1C}(s)$ represents the feedwater to level transfer function at Mode C, and $G_{1C}(s)$ and $G_{2C}(s)$ (Eqs. (15) and (11)) represent the outer and inner control transfer functions, respectively. The validation of each controller with respect to the corresponding

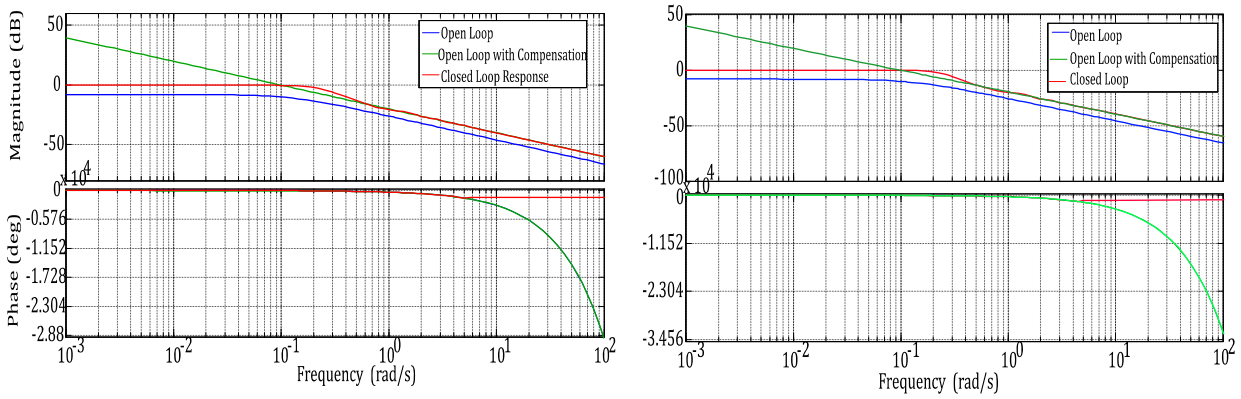

(a) Mode B Inner Loop Bode Plot

(b) Mode C Inner Loop Bode Plot

Fig. 10. Bode plots of inner loop design for schedule controllers at Modes B and C.

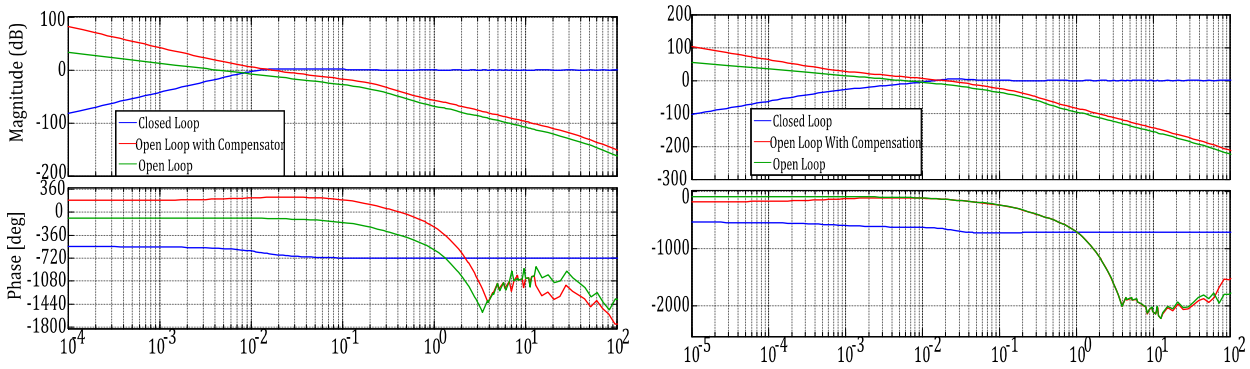

(a) Mode B Outer Loop Bode Plot

(b) Mode C Outer Loop Bode Plot

Fig. 11. Bode plots of outer loop design for scheduled controllers at Modes B and C.

plant model is performed via simulation and is described below. The MATLAB–Simulink model of each mode is used for the simulation study. A step disturbance on the output is provided. In this simulation, each controller for each mode was simulated with its respective plant models. Since each controller is loop shaped based on the model at the respective mode, the linear simulation results showed the expected performance based on the specification. Fig. 12 shows the simulation results of the schedule control scheme; the performance of the schedule control was similar for all modes of boiler operation.

3.3. Robust (QFT) control scheme

A robust control method which works over all the operation modes was designed and verified experimentally using the quantitative feedback theory (QFT) approach. The plant model envelope was specified based on the operating range and different modes of operation. The variations in the model parameters with respect to different modes of boiler operation were translated into uncertain parameters having known interval ranges in the QFT design framework.

3.3.1. Robust specifications

QFT control was designed for both the inner and outer loops. A two degree-of-freedom feedback structure was used for the inner loop, and a simple feedback structure was chosen for the outer loop. Respective specifications are given below.

1. Inner loop specification: For the inner flow loop, its primary goal is to track the flow setpoint coming from the level-control loop. The following are the stability and tracking specifications.

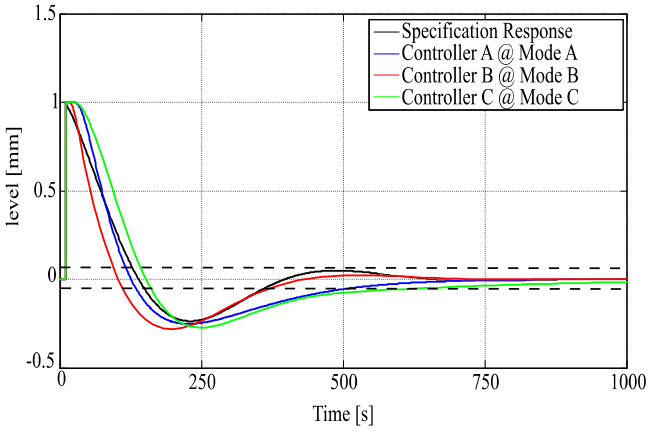

Fig. 12. Closed-loop responses of cascade level control with scheduled controllers.

Robust stability margin: Gain margin $\geq$ 6 dB and phase margin $\geq 45^\circ$. This could be expressed in terms of the closed-loop transfer function as

$$\left|\frac{L(j\omega)}{1+L(j\omega)}\right| \leq 1.2 \tag{16}$$

Tracking specification: The inner loop should track the flow set point provided by the outer loop. The rise time is from 15 to 25 s, peak overshoot is between 0% to 15%, and settling time is 50 s.

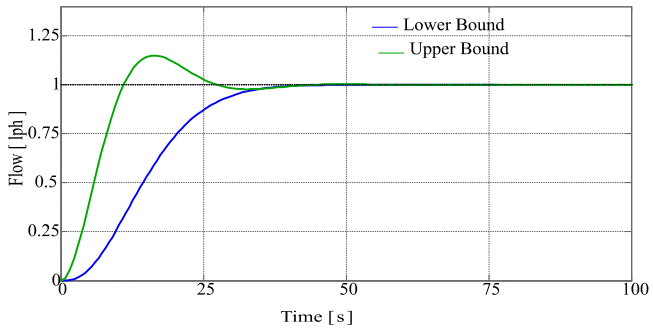

Fig. 13. Tracking specification for the inner flow control loop.

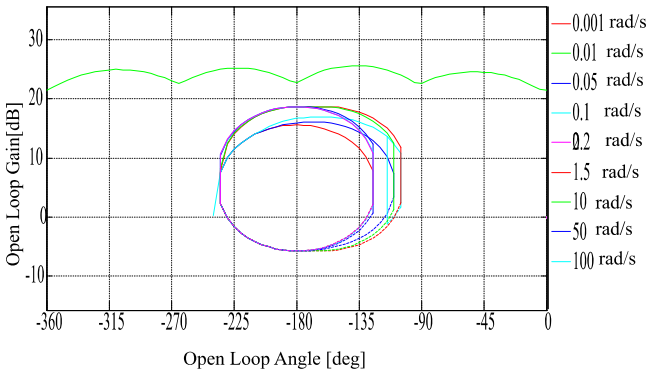

Fig. 14. QFT bounds for the inner flow control loop.

This could be expressed as in Fig. 13. These time-domain specifications can be captured as Upper (T_u) and Lower (T_l) tracking transfer functions given in Eqs. (17) and (18), respectively.

$$T_u(s) = \frac{0.05041}{s^2 + 0.2321s + 0.05041} \tag{17}$$

$$T_l(s) = \frac{0.005042}{s^3 + 0.45s^2 + 0.07843s + 0.005042} \tag{18}$$

2. Outer loop specification: For the outer level loop, disturbance rejection is the fundamental requirement along with robust stability. The following are the stability and disturbance rejection specifications.

Robust stability margin: Gain margin $\geq$ 6 dB and phase margin $\geq$ 45 deg. The closed-loop transfer function is

$$\left| \frac{L(j\omega)}{1 + L(j\omega)} \right| \leq 1.2 \tag{19}$$

Disturbance rejection: The output disturbance rejection specification states that disturbance is kept to 5% of the initial effect of disturbance in 500 s. The time-domain response of the disturbance rejection specification is given in Fig. 5, where α_p represents the disturbance magnitude at the time t_x. The same can be mathematically represented by a second-order transfer function model $W_d(j\omega)$ adapted from [41], and is given by Eq. (20). The robust control design objective is to synthesize a SISO QFT controller that satisfies the desired disturbance rejection specification across the entire plant set **P**.

$$W_d(j\omega) = \frac{((j\omega)^2 + 0.0061(j\omega))}{((j\omega)^2 + 0.0121(j\omega) + 0.000185)} \tag{20}$$

3.3.2. Design details of two-element QFT control

In the laboratory boiler experimental case study, the operation envelope interval covers all three boiler configurations: Modes A, B, and C.

3.3.2.1. Inner loop. The inner loop for the laboratory boiler is the flow loop; the flow loop process provides the desired flow to the boiler based on the set point. The transfer function model of the pump represents the process in this loop. In this design, the pump transfer function for the entire operating envelope is considered. $\mathbf{P_2(s)}$ represents a set of pump models such that $P_2 \in \mathbf{P_2}$ represents elements of the plant set. The pump transfer function is given in Eq. (21).

$$P_2(s) = K \frac{e^{-T_d s}}{T_p s + 1} \tag{21}$$

where $K = [0.3, 0.41]$, $T_p = [5, 10]$, and $T_d = [3, 6]$. QFT bounds are generated based on the inner loop specification, as shown in Fig. 14. The control and pre-filter loop shapes in the Nichols Chart to satisfy bounds are shown in Fig. 15. Validations of the design are shown in Fig. 16.

$$G_{2qft}(s) = 2.9 + \frac{0.31}{s} \tag{22}$$

$$F_{2qft}(s) = \frac{0.38}{(s + 0.38)} \tag{23}$$

where $G_{2qft}(s)$ and $F_{2qft}(s)$ in Eqs. (22) and (23) represent the inner loop controller and prefilter transfer functions, respectively.

3.3.2.2. Outer loop design. The feedwater to flow transfer function of the entire operating regime was identified and expressed in a linear parameter variation form. Eqs. (24) and (25) show the feedwater to level transfer functions used for the QFT design. QFT bounds were generated based on the combination of inner loop and all possible combinations of flow to level transfer functions. The QFT bounds based on plant set and specification are shown in Fig. 17. A QFT controller (see Eq. (26)) was designed to satisfy these bounds and is shown in Fig. 18.

The plant model set (feedwater to level) is denoted as $\mathbf{P_1}$, where $\mathbf{P_1}$ represents the set of models that encompass the laboratory boiler operation regime. It is expressed in terms of two structures.

Structure I

$$P_1(s) = \frac{K}{s(s + a)(s + b)} \tag{24}$$

where $K = [3.2 \times 10^{-5}, 1.53]$, $a = [0.002, 7 \times 10^{-3}]$, and $b = [0.004, 318]$ represent the parameter variations.

Structure II

$$P_1(s) = \frac{Ke^{-T_d s}}{(s + a)(s + b)(s + c)} \tag{25}$$

where $K = [1.53 \times 10^{-5}, 0.1874]$, $a = [0, 0.0045]$, $b = [0.0053, 0.7583]$ and $c = [0.1, 52]$ represent the parameter variations.

Outer-Loop QFT Controller

$$G_{1qft}(s) = \frac{0.17968(s + 0.002996)(s + 3.146)}{s(s + 1.043)(s + 0.1658)} \tag{26}$$

where $G_{1qft}(s)$ represents the outer-loop QFT controller.

Validations of the QFT design using the frequency domain are shown in Fig. 19. However, QFT design validation is only completed with time-domain simulations; Fig. 20 shows the linear simulation results for the plant envelope. The time-domain validation of the QFT controller design was performed, and results are presented. A unit step disturbance at the output was provided to validate this controller via time-domain simulation. A single,

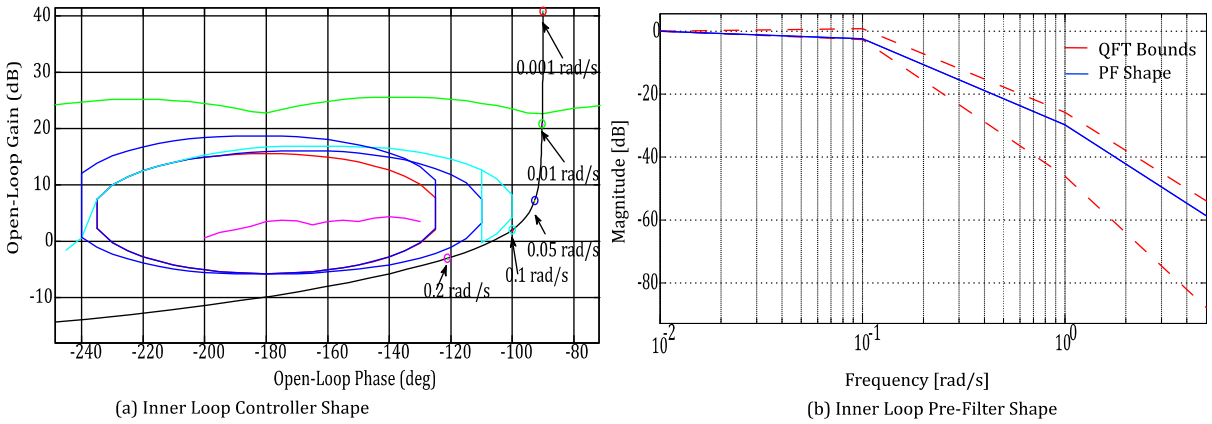

(a) Inner Loop Controller Shape (b) Inner Loop Pre-Filter Shape

Fig. 15. QFT controller and pre-filter design for the inner flow loop. (Black is loop-shaped open loop response ($L_0(jw)$); other colours are QFT bounds at respective indicated frequencies) (Blue is shaped filter and red is QFT bounds). (For interpretation of the references to colour in this figure legend, the reader is referred to the web version of this article.)

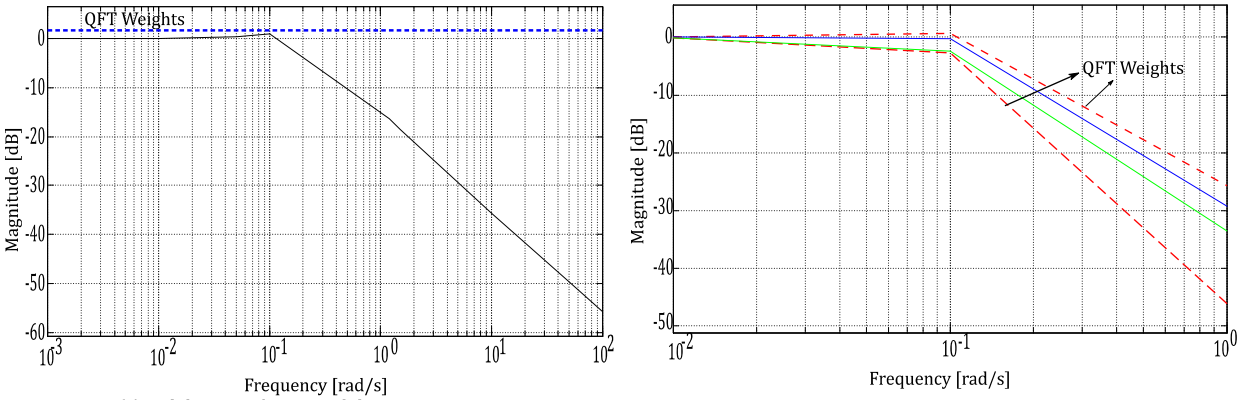

(a) Stability Specification Validation (b) Tracking Specification Validation

Fig. 16. Frequency domain validation of the QFT design for the inner flow loop. (For interpretation of the references to colour in this figure legend, the reader is referred to the web version of this article.)

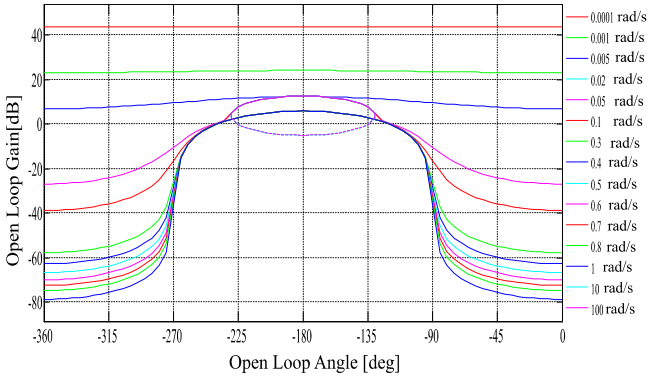

Fig. 17. QFT bounds for the outer level control loop in the cascade structure.

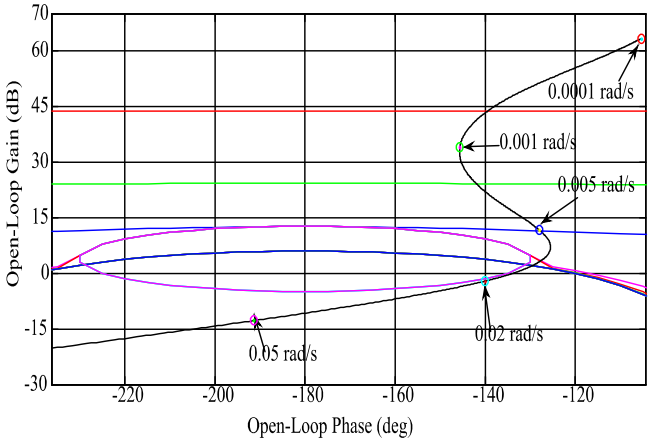

Fig. 18. QFT controller design for the outer level loop. (Black is the loop-shaped open-loop response ($L_0(jw)$); other colours are QFT bounds at respective indicated frequencies). (For interpretation of the references to colour in this figure legend, the reader is referred to the web version of this article.)

robust QFT control provides the robust performance over the entire transfer function set, as shown in Fig. 20. In this simulation, each model was simulated with a QFT based controller, and the design was validated based on the time-domain specification.

4. Experimental results and discussion

This section presents the experimental results of the controllers that were discussed in the previous section. All the controller designs were realized in NI LabVIEW [37]; they interface with instruments and actuators of the boiler system. The performance of each controller was evaluated and is presented in this section. The steam load/demand disturbance was mimicked by a disturbance bypass valve in our lab-scale boiler experimental setup. A 1/2 turn disturbance pulse (between 200 and 300 s) in

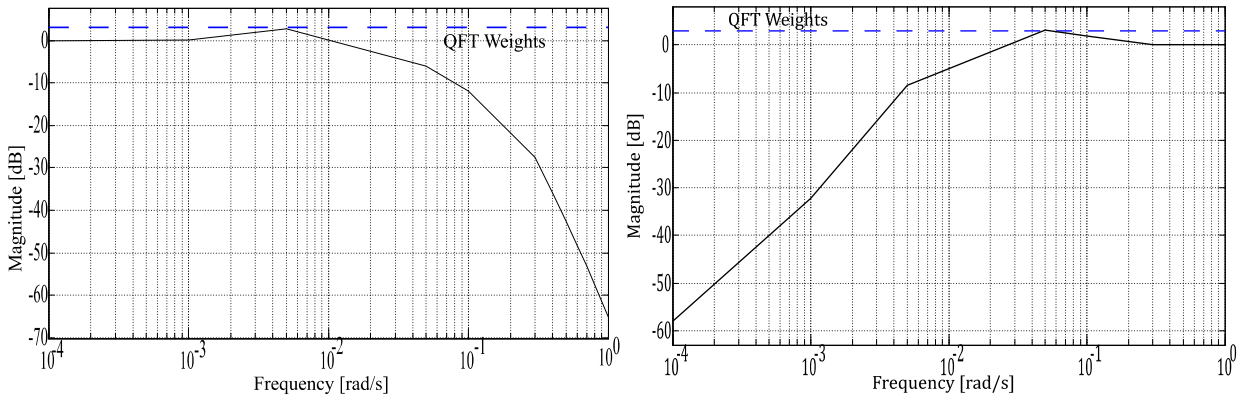

(a) Outer Loop Stability Specification Validation

(b) Outer Loop Disturbance Rejection Specification Validation

Fig. 19. Frequency domain validation of the QFT design for the outer level loop. (Blue is the QFT weights (spec) and black is the frequency response validation of the closed-loop system). (For interpretation of the references to colour in this figure legend, the reader is referred to the web version of this article.)

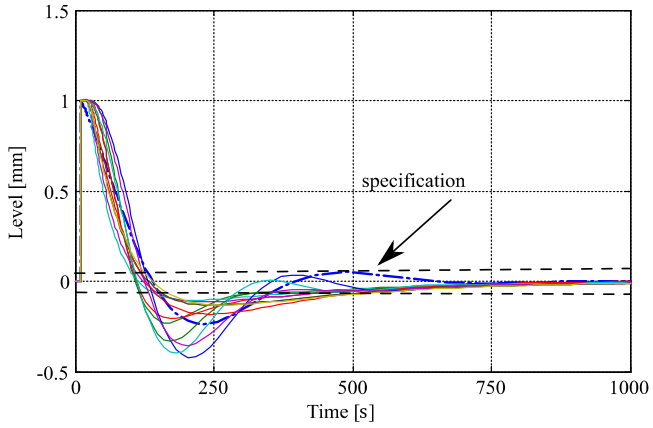

Fig. 20. Time-domain validation of QFT design for the outer level control loop. (Blue dotted line is the specification; other colours are the closed-loop response with various plant models). (For interpretation of the references to colour in this figure legend, the reader is referred to the web version of this article.)

bypass-valve position was applied to emulate an approximately 20% pulsed disturbance in steam-flow. Each controller (i.e., fixed, scheduled, and QFT) was tested separately in all three modes (Mode A, Mode B, and Mode C) of the boiler configuration multiple times with the same disturbance pulse. The performance of each controller regarding disturbance rejection, as well as the control effort of the feed pump, was observed for evaluation and is presented here.

Figs. 21, 22, and 23 show a comparison of the time responses of level, level-error, and controller-effort for all the controllers under investigation in Modes A, B, and C, respectively. Since controller designs of the fixed control and schedule control schemes are identical for Mode A, only one experiment was performed; the same data were used in the analysis for both fixed and schedule control schemes. Hence, the blue line is below the green line in Fig. 21.

The performance of each controller was analysed and compared to evaluate the proposed robust control scheme based on drum level error. The control performance metrics (based on error index) used in this study are 1-norm, 2-norm, ∞-norm, ISE (Integral Square Error), and IAE (Integral Absolute Error). The formulation for these error indices used in this work are given in Eqs. (27) to (31), respectively.

$$\|e\|_1 = \left(\sum_{i=1}^{n} |e_i|\right) \tag{27}$$

$$\|e\|_2 = \left(\sum_{i=1}^{n} e_i^2\right)^{1/2} \tag{28}$$

$$\|e\|_\infty = \max_i(e_i) \tag{29}$$

$$ISE = \int |e|^2\, dt \tag{30}$$

$$IAE = \int |e|\, dt \tag{31}$$

Table 5 shows these error indices for all three control schemes at every operational mode; Table 6 indicates the improvement shown by the proposed QFT robust control scheme over the fixed and scheduled control schemes.

Table 7 shows control-effort analysis for each control scheme. The performance of the fixed controller is poor in all modes, as expected. The QFT controller shows ~20% improvement with respect to fixed control (i.e., the commonly used fixed-load industrial control scheme). The improvement of the proposed QFT control scheme is at the cost of ~15% more than the control effort. From an industrial point of view, this indicates the requirement of additional power in actuators such as feedwater pump-set, control valves, etc.; however, boiler systems usually have a design margin of ~20% at steady states. Hence, there will not be additional costs associated with actuators. When implementing this approach on the industrial problem, actuator constraints also need to be considered-see the authors' study using the QFT approach on an industrial boiler [33]. In the comparison of the QFT controller with the scheduled controller, the QFT controller again showed improved performance for Mode A and Mode C, by ~20% and 17%, respectively. However, for Mode B, the QFT controller shows ~8% inferior performance when compared to the scheduled controller. After further investigation by analysing the frequency responses, it was noted that the scheduled controller has a 10 dB higher low-frequency gain as compared to the QFT controller while operating at mode B. This results in a three-times stronger controller action (by scheduled controller as compared to the QFT controller) at low-frequency range and ~10% stronger controller action at the medium frequency range. This explains the lower error by the scheduled controller in Mode B. To summarize, the 8% poorer performance of the QFT controller was concluded to be because of the higher gain of the schedule controller over low and moderate frequencies. However, the QFT controller has significantly low gain at a higher frequency range due to steeper gain-decay, which can help achieve better sensor-noise rejection by the QFT controller compared to the other two controllers.

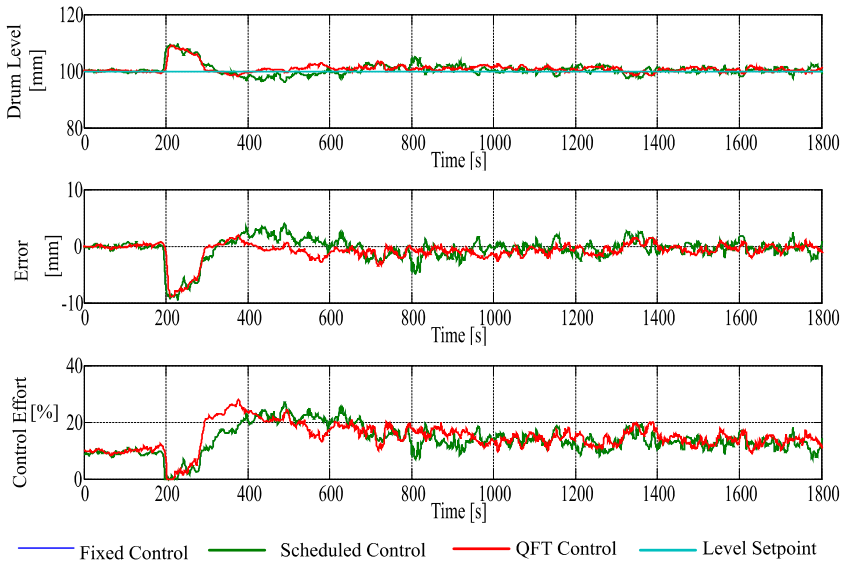

Fig. 21. Comparison of level response, error, and control efforts from experiments with various control schemes on laboratory boiler (Mode A). (For interpretation of the references to colour in this figure legend, the reader is referred to the web version of this article.)

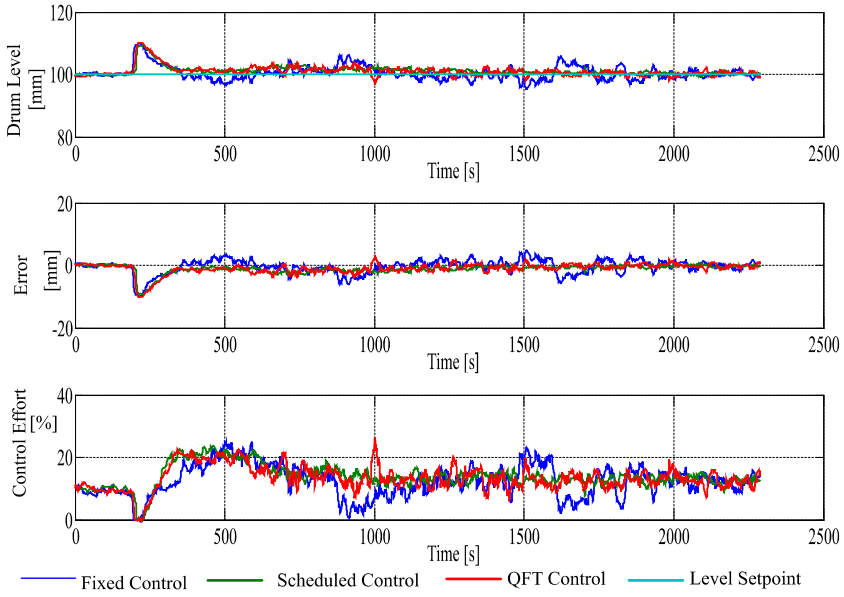

Fig. 22. Comparison of level response, error, and control efforts from experiments with various control schemes on laboratory boiler (Mode B).

Table 5
Error indices.

Mode	Norm 1			Norm 2			Norm inf			ISE			IAE		
	FC	SC	QFT	FC	SC	QFT	FC	SC	QFT	FC	SC	QFT	FC	SC	QFT
A	1.07	1.07	**0.865**	1.05	1.05	**0.91**	1.02	1.02	**0.962**	1.09	1.09	**0.82**	1.07	1.07	**0.86**
B	1.21	**0.86**	0.925	1.13	**0.9**	0.97	1.03	**0.94**	1.032	1.27	**0.79**	0.93	1.21	**0.86**	0.93
C	1.03	1.02	**0.949**	1.07	1.04	**0.89**	1.12	1.02	**0.862**	1.14	1.07	**0.79**	1.03	1.02	**0.95**

FC = Fixed Control, SC = Schedule Control, and QC = QFT control.

5. Conclusions

In this paper, a QFT two-element control scheme was proposed. An experimental case study on a laboratory-scale boiler with a proposed controller and other industrial control schemes was presented, and comparison results are presented in this work. The experimental results show that the proposed QFT robust controller outperforms both fixed and scheduled control schemes in terms of control performance and control-effort metrics. The proposed single QFT controller outperformed a fixed control scheme across the entire wide-range operations (i.e., across all three modes) by ∼20%. In addition, the proposed controller performed better or equivalent to the scheduled controller for most of the wide range of operations (i.e., Modes A and C) by ∼20%. However, the performance of the proposed controller was slightly inferior to the scheduled controller by ∼9% during operational Mode B. This can be overcome by resynthesizing

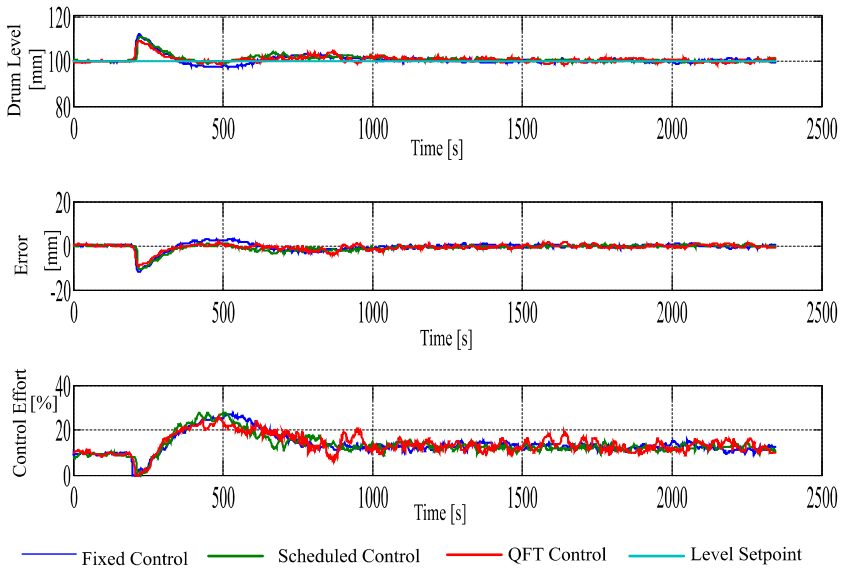

Fig. 23. Comparison of level response, error, and control efforts from experiments with various control schemes on laboratory boiler (Mode C).

Table 6
Error analysis.

Mode	% QFT improvement over FC	% QFT improvement over SC
A	19.81	19.81
B	22.37	−8.96
C	21.30	16.11

FC = Fixed Control, SC = Schedule Control.

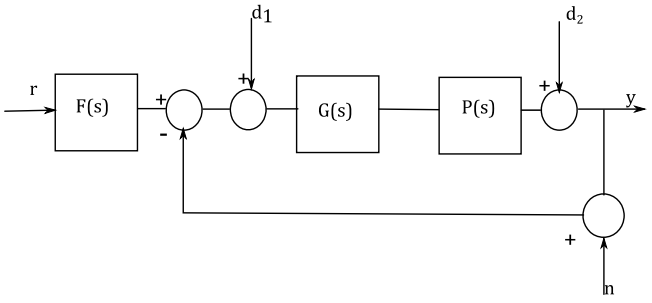

Fig. 24. Two-degree-of-freedom feedback structure used in QFT [34].

the proposed QFT controller by an increasing order of magnitude of the controller. However, considering the advantage of implementing only a single QFT controller working well across a wide range of operation against the complexity of implementing a scheduled controller in a real-time industrial application, it can be concluded that the proposed QFT based robust control scheme promises to accomplish improved performance of boiler-drum level control across a wide-range operational load envelope. Beyond, as the next steps, we propose to continue this research investigation further to (a) extend the proposed QFT robust control scheme to full-range industrial three-element control structures, and (b) explore a robust multivariable control scheme in drum-type boilers.

Acknowledgements

Authors thank GE Power, HTC, Hyderabad to permit first author to carry out his PhD research work as an external research scholar, and also to GE Global Research Centre, Bangalore to permit second author as his co supervisor at IIT Bombay.

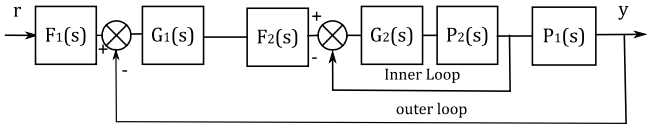

Fig. 25. The cascaded two-degree-of-freedom feedback structure used in QFT [31].

Declaration of competing interest

The authors declare that they have no known competing financial interests or personal relationships that could have appeared to influence the work reported in this paper.

Appendix A. QFT basics

The basic idea in QFT is to convert the desired controls performance specifications into frequency domain constraint-curves (called QFT bounds) on the Nichols chart (for more details please refer [34,41]). Using any gain-phase loop-shaping method, a controller is then designed to satisfy all the bounds at each design frequency. The aim of QFT is to minimize the cost of feedback. Consider a two-degree freedom feedback system configuration (Fig. 24), where $G(s)$ and $F(s)$ are the controller and pre-filter, respectively. The uncertain linear time-invariant plant $P(s)$ is given by $P(s) \in \{P(s,\lambda): \lambda \in \lambda\}$, where $\lambda \in \mathbb{R}^l$ is a vector of plant parameters whose values vary over a parameter box λ

$$\lambda = \{\lambda \in \mathbb{R}^l : \lambda_i \in \underline{\lambda_i}, \overline{\lambda_i}, \underline{\lambda_i} \leq \overline{\lambda_i}, i = 1, \ldots, l\}$$

This gives rise to a parametric plant family or set

$$\boldsymbol{P} = \{P(s,\lambda): \lambda \in \lambda\}$$

The open loop transfer function $L(s,\lambda)$ is defined by Eq. (32), and the nominal open loop transfer function $L_0(s)$ is defined by Eq. (33).

$$L(s,\lambda) = G(s)P(s,\lambda) \tag{32}$$

$$L_0(s) = G(s)P(s,\lambda_0) \tag{33}$$

The objective in QFT is to synthesize $G(s)$ and $F(s)$ such that the various stability and performance specifications are met for

Table 7
Control effort analysis.

Mode	Norm 1			Norm 2			Norm_{inf}			% Control effort of QFT over FC	% Control effort of QFT over SC
	FC	SC	QFT	FC	SC	QFT	FC	SC	QFT		
A	1	**0.998**	1	1.01	1.01	**0.99**	1	**0.997**	1.005	−0.169	−0.169
B	1.03	1.02	**0.95**	1.03	1.01	**0.97**	1	**0.912**	1.086	−2.049	1.963
C	0.99	1.133	**0.88**	1.01	1.1	**0.89**	1.02	1.102	**0.879**	−14.276	−25.968

FC = Fixed Control, SC = Schedule Control, and QC = QFT control.
ϕ Negative number indicates more control effort by QFT controller.

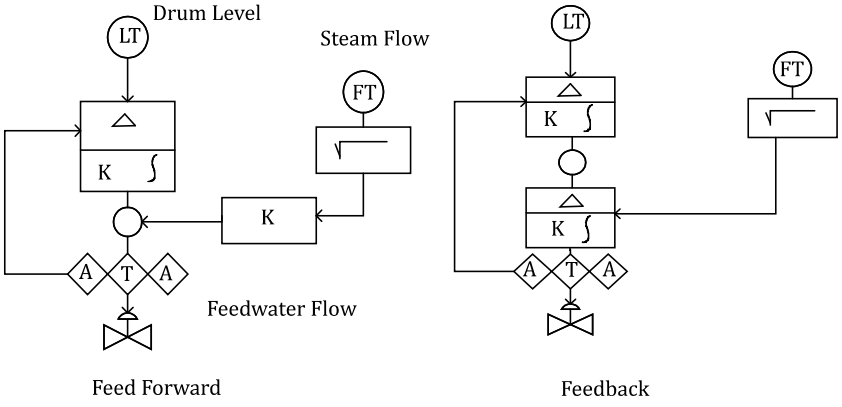

Fig. 26. Structures of two-element control of drum level [9].

all $P(s) \in \boldsymbol{P}$. In general, the following specifications are considered in QFT:

1. Robust stability margin

$$\left|\frac{L(j\omega)}{1+L(j\omega)}\right| \leq \omega_s \tag{34}$$

2. Robust tracking performance

$$|T_L(j\omega)| \leq \left|\frac{F(j\omega)L(j\omega)}{1+L(j\omega)}\right| \leq |T_U(j\omega)| \tag{35}$$

3. Robust input disturbance rejection performance

$$\left|\frac{G(j\omega)}{1+L(j\omega)}\right| \leq \omega_{d_i}(w) \tag{36}$$

4. Robust output disturbance rejection performance

$$\left|\frac{1}{1+L(j\omega)}\right| \leq \omega_{d_o}(w) \tag{37}$$

In practice, the objective is to satisfy the given specifications over a finite design frequency set Ω. The main steps of QFT design specifications are

1. **Generating templates**: For a given uncertain plant $P(s) \in \boldsymbol{P}$, at each design frequency $\omega_i \in \Omega$, calculate the value set of the plant $P(j\omega_i)$ in the complex plane.
2. **Computation of QFT bounds**: For each design frequency ω_i, calculate the stability margins and performance bounds using the stability and performance specifications and plant templates. The bound at ω_i is denoted as $B_i(\angle L_0(j\omega), \omega_i)$ or simply B_i
3. **Design of Controller**: Design a controller $G(s)$ such that

- The bound constraints at each design frequency ω_i are satisfied.
- The nominal closed loop system is stable.

4. **Design of Prefilter**: Design a prefilter $P(s)$ such that the robust tracking specifications are satisfied.

Cascade QFT basics

An overview of the cascade QFT design procedure is described. For theory and details of different approaches, please refer to [31, 41]. Two uncertain parametric models, $\mathbf{P_1}$ and $\mathbf{P_2}$, represent the set of uncertain plants, similar to that explained in the previous section (Fig. 25). The design of the inner loop is straightforward. However, for the outer loop, some additional computations are required. The closed loop inner transfer function T_2 as shown in Eq. (38).

$$T_2(s) = F_2(s)\frac{P_2(s)G_2(s)}{(1+P_2(s)G_2(s))} \tag{38}$$

The effective plant for the outer loop design is $P_{12}(s) = P_2(s)T_2(s)$, and $\mathbf{P_{12}}$ represents the set of uncertain effective open loop plants, which is computed with all possible combinations of P_2 and T_2. Once this effective open loop set is derived, then the QFT method falls back to the same procedure discussed in the previous section, with $\mathbf{P_{12}}$ as the uncertain plant set.

Appendix B. Industrial two element control schemes

Two variants of two-element control are generally practised in industry. One variant uses steam measurement as the second element, which acts as a feedforward control. A feedforward loop is implemented in the steam flow outlet. This control strategy holds the water level at a set point. During the shrink and swell period, proper tuning action is required to balance the effects of steam flow and drum water level. The second variant uses feedwater flow as the second element, and it is structured as a cascade loop with level control as an outer loop and flow control as an inner loop. This scheme helps to counter any unpredictable change in the feedwater line before affecting the primary variable. This structure is typically used in low-power operations and is shown in Fig. 26.

References

[1] Bird L, Milligan M, Lew D. Integrating Variable Renewable Energy: Challenges and Solutions, (2013) 14. doi:NREL/TP-6A20-60451.

[2] Martinot E. How is Denmark integrating and balancing Renewable energy today? Marinot 2015;1–5, http://www.martinot.info/Martinot_DK_Integration_2015.pdf (accessed August 10, 2016).

[3] Ulbig A. Grid integration challenges of renewable energy sources and prospective solutions. In: Swiss Fed. Inst. Technol. Zurich.. 2013, https://www.ethz.ch/content/dam/ethz/special.../energy.../131030_FiER_Ulbig.pdf (accessed August 10, 2016).

[4] Shafiullah GM, Amanullah MT Oo, Shawkat Ali ABM, Wolfs P. Potential challenges of integrating large-scale wind energy into the power grid–A review. Renew Sustain Energy Rev 2013;20:306–21. http://dx.doi.org/10.1016/j.rser.2012.11.057.

[5] Botterud A. Grid integration of renewable energy. Int Electrotech Commun 2014;2:1–34. http://dx.doi.org/10.1007/978-3-319-30427-4.

[6] Eser P, Singh A, Chokani N, Abhari RS. Effect of increased renewables generation on operation of thermal power plants. Appl Energy 2016;164:723–32. http://dx.doi.org/10.1016/j.apenergy.2015.12.017.

[7] Kubik ML, Coker PJ, Barlow JF. Increasing thermal plant flexibility in a high renewables power system. Appl Energy 2015;154:102–11. http://dx.doi.org/10.1016/j.apenergy.2015.04.063.

[8] Tan W, Marquez HJ, Chen T, Liu J. Analysis and control of a nonlinear boiler-turbine unit. J Process Control 2005;15:883–91. http://dx.doi.org/10.1016/j.jprocont.2005.03.007.

[9] Dukelow SG. The control of boilers. Instrument Society of America; 1991.

[10] Duncan RL, Brown HW. Root cause analysis of outages in combined-cycle power plants. In: 4 Heat Transf. Electr. Power.. 1984, http://dx.doi.org/10.1115/84-gt-12.

[11] Tan W, Marquez HJ, Chen T. Multivariable robust controller design for a boiler system. IEEE Trans Control Syst Technol 2002;10:735–42. http://dx.doi.org/10.1109/tcst.2002.801787.

[12] Chen PC, Shamma JS. Gain-scheduled L1-optimal control for boiler-turbine dynamics with actuator saturation. J Process Control 2004;14:263–77. http://dx.doi.org/10.1016/s0959-1524(03)00040-4.

[13] Tan W, Liu J, Fang F, Chen Y. Tuning of PID controllers for boiler-turbine units. ISA Trans 2004;43:571–83. http://dx.doi.org/10.1016/s0019-0578(07)60169-4.

[14] Kim WG, Moon UC, Lee SC, Lee KY. Application of dynamic matrix control to a boiler-turbine system. In: IEEE Power Eng. Soc. Gen. Meet. 2005, Vol. 2. 2005, p. 1595–600. http://dx.doi.org/10.1109/PES.2005.1489441.

[15] Xu M, Li S, Cai W. Cascade generalized predictive control strategy for boiler drum level. ISA Trans 2005;44:399–411. http://dx.doi.org/10.1016/S0019-0578(07)60212-2.

[16] Li ZJ, Li ZX, Tan W, Liu JZ. Constrained dynamic matrix control for a boiler-turbine unit. In: Int. Conf. Mach. Learn. Cybern.. 2006, http://dx.doi.org/10.1109/icmlc.2006.258396.

[17] Labibi B, Marquez HJ, Chen T. Decentralized robust PI controller design for an industrial boiler. J Process Control 2009;19:216–30. http://dx.doi.org/10.1016/j.jprocont.2008.04.013.

[18] Zheng K, Bentsman J, Taft CW. Full operating range robust hybrid control of a coal-fired boiler/turbine unit. J Dyn Syst Meas Control 2008;130:41011. http://dx.doi.org/10.1115/1.2907367.

[19] Moon UC, Lee KY. An adaptive dynamic matrix control with fuzzy-interpolated step-response model for a drum-type boiler-turbine system. IEEE Trans Energy Convers 2011;26:393–401. http://dx.doi.org/10.1109/tec.2011.2116023.

[20] Morilla F. Benchmark for PID control based on the Boiler Control Problem. IFAC Proc 2012;45:346–51. http://dx.doi.org/10.3182/20120328-3-it-3014.00059.

[21] Chen PC. Multi-objective control of nonlinear boiler-turbine dynamics with actuator magnitude and rate constraints. ISA Trans 2013;52:115–28. http://dx.doi.org/10.1016/j.isatra.2012.08.002.

[22] Aliakbari S, Ayati M, Osman JHS, Sam YM. Second-order sliding mode fault-tolerant control of heat recovery steam generator boiler in combined cycle power plants. Appl Therm Eng 2013;50:1326–38. http://dx.doi.org/10.1016/j.applthermaleng.2012.04.054.

[23] Moradi H, Abbasi MH, Moradian H. Improving the performance of a nonlinear boiler–turbine unit via bifurcation control of external disturbances: a comparison between sliding mode and feedback linearization control approaches. Nonlinear Dynam 2016;85:229–43. http://dx.doi.org/10.1007/s11071-016-2680-x.

[24] Kong X, Liu X, Lee KY. Nonlinear multivariable hierarchical model predictive control for boiler-turbine system. Energy 2015;93:309–22. http://dx.doi.org/10.1016/j.energy.2015.09.030.

[25] Ławryńczuk M. Nonlinear predictive control of a boiler-turbine unit: A state-space approach with successive on-line model linearisation and quadratic optimisation. ISA Trans 2017;67:476–95. http://dx.doi.org/10.1016/j.isatra.2017.01.016.

[26] Gan B, Lv H. Research on drum water level control of marine auxiliary boiler based on ADRC. Polish Marit Res 2018;25:35. http://dx.doi.org/10.2478/pomr-2018-0071.

[27] Klaučo M, Kvasnica M. Control of a boiler-turbine unit using MPC-based reference governors. Appl Therm Eng 2017;110:1437–47. http://dx.doi.org/10.1016/j.applthermaleng.2016.09.041.

[28] Sunil PU, Desai K, Barve J, Nataraj PSV. Lab scale boiler setup for process control research and education. IFAC-PapersOnLine 2017;50:2373–8. http://dx.doi.org/10.1016/j.ifacol.2017.08.428.

[29] Desai K, Sunil PU, Barve J, Nataraj PSV. Modeling and identification of experimental drum type steam boiler. In: 2016 IEEE Annu. India Conf. INDICON 2016. 2017, http://dx.doi.org/10.1109/INDICON.2016.7839057.

[30] Horowitz IM. Synthesis of feedback systems. Academic Press; 1963.

[31] Horowitz I. Survey of quantitative feedback theory (QFT). Internat J Robust Nonlinear Control 2001;11:887–921. http://dx.doi.org/10.1002/rnc.637.

[32] Horowitz I, Sidi M. Synthesis of feedback systems with large plant ignorance for prescribed time-domain tolerances†. Internat J Control 1972;16:287–309. http://dx.doi.org/10.1080/00207177208932261.

[33] Sunil PU, Barve J, Nataraj PSV. A robust heat recovery steam generator drum level control for wide range operation flexibility considering renewable energy integration. Energy 2018;163:873–93. http://dx.doi.org/10.1016/j.energy.2018.08.167.

[34] Horowitz I. Quantitative feedback design theory (QFT). QFT Publications; 1993.

[35] Houpis CH. Quantitative feedback technique (QFT): Bridging the gap. In: RTO SCI Lect. Ser. Robust Integr. Control Syst. Des. Methods 21st Century Mil. Appl.. 2003, p. 1–56, papers2://publication/uuid/7144716E-57F0-4CC0-A97E-9B3BDF6B87E3.

[36] Garcia-Sanz M. Robust control engineering: Practical QFT solutions. First, CRC Pressc; 2017.

[37] National Instruments, Getting Started With LabView, North. (2013). doi:http://dx.doi.org/10.1007/BF02798849.

[38] Kopasakis G. Feedback Control Systems Loop Shaping Design With Practical Considerations, Nasa/Tm - 2007-215007. (2007). https://ntrs.nasa.gov/archive/nasa/casi.ntrs.nasa.gov/20070034948.pdf.

[39] Mathworks, Control System Toolbox, Control Syst. Toolbox Doc. (2017). https://www.mathworks.com/help/control/ (accessed August 20, 2016).

[40] MathWorks, Simulink-Simulation and Model-Based Design, (2017). https://in.mathworks.com/help/simulink/index.html (accessed January 28, 2017).

[41] Houpis CH, Garcia-Sanz M, Rasmussen SJ. Quantitative feedback theory: Fundamentals and applications. CRC; 2006.